Journal of Materials Chemistry C

RSC Publishing

PAPER

View Article Online
View Journal | View Issue

Cite this: J. Mater. Chem. C, 2013, 1, 5756

Fluorescent micelles based on hydrophobically modified cationic cellulose for sensing trace explosives in aqueous solutions

Lingzhi Zhang,[a] Chengcheng Zhao,[a] Jinping Zhou*[ab] and Tetsuo Kondo[b]

Received 14th April 2013
Accepted 28th June 2013

DOI: 10.1039/c3tc30689e

www.rsc.org/MaterialsC

Amphiphilic cationic cellulose derivatives with different long alkyl chains as hydrophobic segments were synthesized. They can self-assemble into cationic micelles in distilled water. The structure and properties of the micelles were characterized by elemental analysis, FT-IR, ^{1}H NMR, ζ-potential measurements, DLS, TEM, and fluorescence spectroscopy. The hydrophobic cores of the micelles were used to load a hydrophobic dye (4,7-bis[4-(1,2,2-triphenylvinyl)phenyl]benzo-2,1,3-thiadiazole, BTPETD) and exhibited a stable photoluminescence. The fluorescence emission can quantitatively and sensitively respond to 2,4-dinitrophenol (DNP) and picric acid (PA) due to the electron transfer between BTPETD and the explosives, and the limit of detection was 200 and 50 nM for DNP and PA, respectively. The novel hydrophobically modified cationic cellulose micelles have the potential to prepare feasible, sensitive and stable sensor systems for detecting explosives in aqueous solutions.

1 Introduction

There has been an immense research interest in the detection of trace explosives, which is very important for public security and pollution problems for humans and ecosystems.[1] Currently, many techniques and sensors have been reported for the improvement of trace detection.[2] The need for the sensitive detection of explosive compounds of low-volatility has resulted in an intense focus on fluorescence methods, which include nanotechnology-based sensors,[3–5] amplifying fluorescent polymer-based sensors,[6,7] electrochemistry-based sensors,[8,9] fluorescence resonance energy transfer (FRET) sensors[10,11] and fluorescence quenching sensors.[12–16] Among these methods, fluorescence quenching sensors have been proven to be very simple and sensitive tools to detect 2,4,6-trinitrotoluene (TNT) and other nitro-based explosives. Fluorescence quenching refers to any process that decreases the fluorescence intensity of a sample. A variety of molecular interactions can result in quenching, including excited-state reactions, molecular rearrangements, energy transfer, ground-state complex formation, collisional quenching, and so on. Mostly, quenching is achieved through an electron transfer donor–acceptor mechanism.[14] Yang *et al.* prepared a novel chemosensing device based on poly(acrylic acid) brush films.[2] Quaternary ammonium tetraphenylene derivatives were self-assembled on the brushes and displayed excellent photoluminescent properties and a highly fluorescence quenching sensitivity and selectivity in the presence of TNT. Xu *et al.* designed and synthesized strong donor–acceptor conjugated polymers for the highly selective and sensitive detection of TNT and picric acid (PA) in aqueous solutions.[17] Nitroaromatics have good capacities in accepting electrons. However, dyes used as electron donors in fluorescence quenching are hydrophobic, which limits their use in aqueous systems. Therefore, micelles of cellulose derivatives were used to load the dyes into their hydrophobic cores.[18]

As is known, cellulose, due to its outstanding merits such as abundance, low cost, safety, non-toxicity, biocompatibility, biodegradability and easy modification, has received increasing attention.[19–21] An increasing interest has been focused on polymer micelles based on hydrophobically modified cellulose and cellulose derivatives,[18,22–24] because they not only solubilize and stabilize the hydrophobic dye but also decrease the eventual high toxicity to the environment and healthy cells.[25] Previously, self-assembled micelles based on hydrophobically modified quaternized cellulose (HMQC) have been obtained and used as hydrophobic drug delivery systems.[26]

In this work, we attempt to develop cellulose-based micelles for the ultrasensitive and selective detection of explosives. HMQC derivatives with different long alkyl chains were firstly synthesized, and then self-assembled into micelles in water. A tetraphenylethene derivative (d-TPE), a hydrophobic fluorescence probe, was loaded into the hydrophobic core of the micelles and exhibited excellent luminescent properties. As an electron donor, the d-TPE molecule is a promising candidate for nitroaromatics detection, because nitroaromatics have a good capacity to accept electrons and lower the energy of the empty

[a]Department of Chemistry, Wuhan University, Wuhan 430072, China. E-mail: zhoujp325@whu.edu.cn; Fax: +86-27-68754067; Tel: +86-27-87219274

[b]Graduate School of Bioresource and Bioenvironmental Sciences, Kyushu University, 6-10-1 Hakozaki, Higashi-ku, Fukuoka 812-8581, Japan

π* orbitals of d-TPE, causing quenching.[27] For example, the energy gap obtained absorption spectrum (E_{opt}), the highest occupied molecular orbital (HOMO), the lowest unoccupied molecular orbital (LUMO), and the theoretically calculated energy gap (E_{gap}) for 4,7-bis[4-(1,2,2-triphenylvinyl)phenyl]-benzo-2,1,3-thiadiazole (BTPETD) were 2.55, −5.31, −2.47, and 2.84 eV, respectively.[28] Therefore, the fluorescence intensity could be quenched with various concentrations of explosives, leading to the detection of explosives.

2 Materials and methods

2.1 Materials

Cellulose (cotton linter pulp) was supplied by the Hubei Chemical Fiber Group Ltd. (Xiangyang, China), and the viscosity average molecular weight (M_η) was determined by viscosimetry to be 1.04×10^5 g mol^{-1}. (3-Chloro-2-hydroxypropyl)trimethylammonium chloride (CHPTAC) aqueous solution (69 wt%) was purchased from the Guofeng Fine Chemical Co. Ltd. (Shandong, China), and used as an etherifying reagent without further purification. Picric acid (PA) was purchased from the Xilong Chemical Co. Ltd. (Guangdong, China). 2,4-Dinitrotoluene (DNT) and the TNT–methanol solution (0.99 mg mL^{-1}) were purchased from the Aladdin Industry Corporation (Shanghai, China). Octyl bromide, dodecyl bromide, cetyl bromide, *p*-nitrophenol (NP), *p*-nitrotoluene (NT), 2,4-dinitrophenol (DNP), fluorescein and the other reagents of analytical grade were supplied by the Sinopharm Chemical Reagent Co. Ltd. (Shanghai, China), and used without further purification.

The hydrophobic fluorescence probe, BTPETD, was synthesized according to ref. 28. ^{1}H NMR (300 MHz, $CDCl_3$), δ (TMS, ppm): 7.76 (d, 4H), 7.67 (s, 2H), 7.21–7.07 (m, 34H). ^{13}C NMR (300 MHz, $CDCl_3$), δ (TMS, ppm): 154.3, 144.0, 141.8, 140.8, 135.5, 132.8, 131.7, 128.6, 128.0, and 126.7.

2.2 Synthesis of QC

Quaternized cellulose (QC) was prepared according to previous work.[26,29] Briefly, an amount of the CHPTAC aqueous solution (molar ratio of the CHPTAC to the anhydroglucose unit (AGU) of cellulose was 18 : 1) was added drop-wise into a cellulose–NaOH–urea–aqueous solution, and the mixture was stirred at 25 °C for 24 h. The reaction product was neutralized with HCl solution, dialyzed and freeze-dried to obtain the water soluble QC. The nitrogen content of the QC was determined to be 3.06%.

2.3 Synthesis of HMQC

Hydrophobically modified quaternized cellulose (HMQC) was prepared according to our previous work.[26] QC (1.0 wt%) was dissolved in 5.0 wt% of a NaOH aqueous solution and stirred at 25 °C for 3 h. Then an amount of a long chain alkyl bromide was added drop-wise into the QC solution, and the mixture was stirred at 60 °C for 6 h. Finally, the solution was precipitated and washed with ethanol, and dried under a vacuum at 40 °C. As shown in Table 1, a series of HMQC derivatives (QCO, QCD and QCC) were obtained by changing the molar ratio of the long chain alkyl bromide to the AGU of the QC.

2.4 Formation of HMQC micelles

The micelles were prepared by a dialysis method.[30] The HMQC derivatives were dispersed in distilled water at the concentration of 1.5 mg mL^{-1}, and then dialyzed against distilled water for 24 h using a dialysis tube (M_w cutoff 8000), and the distilled water was replaced every 4 h. Finally, a concentration of 1.0 mg mL^{-1} HMQC was obtained by partial evaporation under a vacuum, to remove the water.

2.5 Preparation of fluorescent micelles

BTPETD encapsulated HMQC micelles were prepared by slowly adding the BTPETD–DMSO solution (0.25 mg mL^{-1}, 2.4 mL) into the aqueous solution of the HMQC micelles (1.50 mg mL^{-1}, 3.0 mL) under vigorous stirring. The mixture solution was dialyzed against distilled water for 24 h using a dialysis tube (M_w cutoff 8000), and the distilled water was replaced every 4 h. Then the solution was filtered through a 0.45 μm microfilter to eliminate the non-incorporated BTPETD. The concentration of the BTPETD in the HMQC micelles solution was determined by a UV-vis spectrometer at 426 nm. The resulting solution was then diluted with a volume of water to make the concentration of BTPETD approximately 0.01 mg mL^{-1}. The loading efficiency (LE, %) and loading capacity (LC, %) of the BTPETD in the HMQC micelles were determined by the following equations:

$$\text{LE}\ (\%) = W_{dye}/W_0 \times 100 \quad (1)$$

$$\text{LC}\ (\%) = W_{dye}/(W_{dye} + W_{polymer}) \times 100 \quad (2)$$

where $W_{polymer}$ was the weight of the HMQC polymer fed initially, W_0 was the weight of the dye (BTPETD) fed initially, and W_{dye} was the weight of the dye loaded into the micelles.

2.6 Characterization

The nitrogen content (*N*%) of the QC and HMQC derivatives was measured with an elemental analyzer (CHN-O-Rapid, Foss Hera us GmbH, Hanau, Germany). The degree of substitution of the quaternary ammonium group (DS_Q) was determined by the nitrogen content of the QC (N_{QC}%), and calculated to be 0.53 according to the following equation:

$$DS_Q = 162 \times N_{QC}\% \Big/ (14 - 151.5 \times N_{QC}\%) \quad (3)$$

The DS values of the hydrophobic long alkyl chain groups (DS_H) were determined by the nitrogen content of the HMQC (N_{HMQC}%), and calculated according to the following equation:

$$DS_H = \left(\frac{DS_Q \times 14}{N_{HMQC}\%} - 248\right) \Big/ (14n) \quad (4)$$

where *n* was 8, 12, 16 for the QCO, QCD and QCC derivatives, respectively.

The FT-IR spectra of the QC and HMQC samples were obtained with a Nicolet 170SX Fourier transform infrared spectrometer. The test specimens were prepared by the KBr-disc method. The UV-vis spectra were obtained by using a UV double beam spectrophotometer (UV-6100PCS, China). The

Table 1 Synthesis and physicochemical properties of the HMQC derivatives

Code	Reactants	Molar ratio[a]	N (%)	DS_Q	DS_H	CMC (mg L^{-1})	ζ (mV)	R_h[b] (nm)
QC	—	—	3.06	0.53	0	—	48.4	—
QCO-1	Octyl bromide	6 : 1	2.72	0.53	0.21	648.9	47.1	274.1
QCO-2	Octyl bromide	9 : 1	2.64	0.53	0.30	301.1	48.0	226.5
QCO-3	Octyl bromide	12 : 1	2.57	0.53	0.36	207.0	50.1	172.4
QCD-1	Dodecyl bromide	9 : 1	2.58	0.53	0.23	151.1	51.3	391.0
QCD-2	Dodecyl bromide	12 : 1	2.46	0.53	0.31	126.2	50.7	231.4
QCD-3	Dodecyl bromide	15 : 1	2.39	0.53	0.37	108.6	52.5	207.1
QCC-1	Cetyl bromide	9 : 1	2.56	0.53	0.18	119.5	52.4	322.6
QCC-2	Cetyl bromide	12 : 1	2.42	0.53	0.26	104.6	49.6	246.8
QCC-3	Cetyl bromide	15 : 1	2.29	0.53	0.33	80.6	54.4	229.2

[a] Molar ratio of the long chain alkyl bromide to the AGU of the QC. [b] Hydrodynamic radius (R_h) in distilled water determined by dynamic laser light scattering.

fluorescence experiments were performed on a spectrofluorophotometer (RF-5301pc, Shimadzu, Japan). The fluorescence quantum yields (Φ_F) were determined by a comparative method, using fluorescein as a standard reference with a $\Phi_F = 0.97$, in ethanol.[31]

The ^{1}H NMR measurement of the QC and HMQC samples in D_2O was carried out on a Varian INOVA-600 spectrometer in the proton noise-decoupling mode with a standard 5 mm probe at 25 °C, and the polymer concentration was about 0.1 wt%. The chemical shifts were referenced to the signals of tetramethylsilane (TMS).

The ζ-Potential of the QC and the HMQC micelles in distilled water was measured on a Nano-ZS ZEN3600 (Malvern Instruments, UK) at 25 °C. The dynamic laser light scattering (DLS) for the hydrodynamic radius (R_h) of the HMQC micelles in distilled water was performed on an ALV/DLS/SLS-5000E light scattering goniometer (ALV/CGS-8F, ALV, Germany) with a vertically polarized incident light of wavelength 632.8 nm from a He–Ne laser equipped with an ALV/LSE-5003 light scattering electronics and multiple tau digital correlator. The scattering angle (θ) was 90°. All of the solutions were filtered directly into the light-scattering cells through a 0.45 μm pore size filter (NYL, Whatman, UK). The concentration of the samples for the ζ-potential and DLS measurements was 1.0 mg mL^{-1}. Each test was repeated at least three times and the average value was reported.

The morphological observation of the HMQC micelles was performed with a transmission electron microscope (HR JEM-2100, Japan), using an accelerating voltage of 200 kV. The TEM sample was prepared by dipping a copper grid with a Formvar film into the freshly prepared micelle solution, and then dyed with a 0.01% (*w*/*v*) phosphotungstic acid aqueous solution. After the deposition, the aqueous solution was blotted away with a strip of filter paper and dried in air.

2.7 Determination of critical micelle concentration

Pyrene was used as a hydrophobic fluorescent probe. Aliquots of pyrene solutions (1×10^{-5} M in acetone, 1 mL) were added to containers, and the acetone was allowed to evaporate. Polymer solutions (10 mL) with different concentrations were added to the containers which contained the pyrene residue with a concentration of 1×10^{-6} M. The solutions were kept at room temperature for 24 h to reach the solubilization equilibrium of pyrene in the aqueous phase. The fluorescence spectra were recorded on the spectrofluorophotometer (RF-5301pc, Shimadzu, Japan). The excitation was carried at 337 nm, and the emission spectra were recorded in the range 350 to 600 nm. Both the excitation and emission slit widths were 10 nm. From the pyrene emission spectra, the intensity (peak height) at 381 nm (I_{381}) was analyzed as a function of the polymer concentration. A critical micelle concentration (CMC) value was determined from the intersection of the tangent to the curve at the inflection with the horizontal tangent, through the points at low concentration.

2.8 Fluorescence quenching for explosives detection

The fluorescence quenching of the BTPETD was obtained by the successive addition of aliquots of the analyte solution. 2.0 mL of the BTPETD encapsulated micelles solution was placed in a covered quartz cuvette. The fluorescence spectra of the solution were measured immediately after each addition, with excitation at 415 nm and a slit width of 3 nm. The concentration of the BTPETD for the fluorescence quenching measurements was kept constant at 0.01 mg mL^{-1}.

3 Results and discussion

3.1 Synthesis and structure of HMQC

The hydrophobically modified quaternized cellulose (HMQC) derivatives were obtained by a two-step synthesis as illustrated in Scheme 1. Firstly, the water-soluble QC with a DS of 0.53 was homogeneously synthesized in a NaOH–urea–aqueous solution from cellulose, directly. Then the long chain alkyl bromide was reacted with the residual hydroxyl groups of the cellulose in the NaOH aqueous solutions, to yield the HMQC. The nitrogen content and the DS values of the QC and HMQC derivatives are listed in Table 1. These data show that with an increasing molar ratio of the long chain alkyl group to the AGU of QC, the nitrogen content of the HMQC decreased, while the DS_H value of the samples increased. The longer the chain that reacted with the QC at the same molar ratio, the lower the nitrogen content of the HMQC obtained, causing the decrease of the DS_H value.

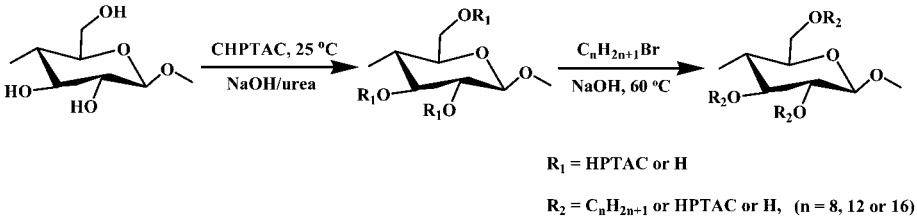

Scheme 1 Synthesis of the QC and HMQC derivatives.

Besides, by introducing the long hydrophobic alkyl chain, the HMQC derivatives were only soluble in dilute distilled water and the mixture of DMSO–H_2O.

Fig. 1 shows the FT-IR spectra of the QC and HMQC samples. From the spectrum of QC, the peaks at 1479 and 1420 cm^{-1} were ascribed to the methyl groups of the substituted ammonium and the stretching vibration of the C–N group, respectively,[29] which demonstrated the introduction of quaternary ammonium groups to the cellulose. Compared with that of QC, the FT-IR spectra of the HMQC derivatives show two apparent peaks at 2921 and 2849 cm^{-1} attributed to the long alkyl chain.[32] Additionally, the peak intensity for the ether bond at 1061 cm^{-1} was stronger than that of the QC, indicating the attachment of the long alkyl chain to the hydroxyl groups of the QC. Moreover, as the molar ratio of the long chain alkyl bromide to the AGU increased, the peaks at 2921 and 2849 cm^{-1} of QCC-1, QCC-2 and QCC-3 enhanced, indicating an increase of the DS_H value.

Fig. 2 shows the ^1H NMR spectra of the QC and HMQC derivatives in D_2O. In the spectrum of QC, the typical signal of the protons in the $(CH_3)_3N^+$ group appeared at 3.14 ppm. In contrast to that of QC, the peak at around 1.33 ppm in the spectra of the HMQC derivatives was assigned to the protons of the methane groups (–O–CH_2–$(CH_2)_{n-2}$–CH_3) of the long alkyl chains. The peak at 0.94 ppm belonged to the protons of the terminal methyl group of the long alkyl chain (–O–CH_2–$(CH_2)_{n-2}$–CH_3). The peak attributed to the methene hydrogen (–O–CH_2–$(CH_2)_{n-2}$–CH_3) of the O-alkyl group was overlapped by the peak of the AGU signals of the cellulose between 3.35 and 4.45 ppm.[33] Besides, as the molar ratio of the long chain alkyl bromide to the AGU increased, the peak at 1.33 ppm of QCC-1, QCC-2 and QCC-3 was enhanced, indicating the increase in the

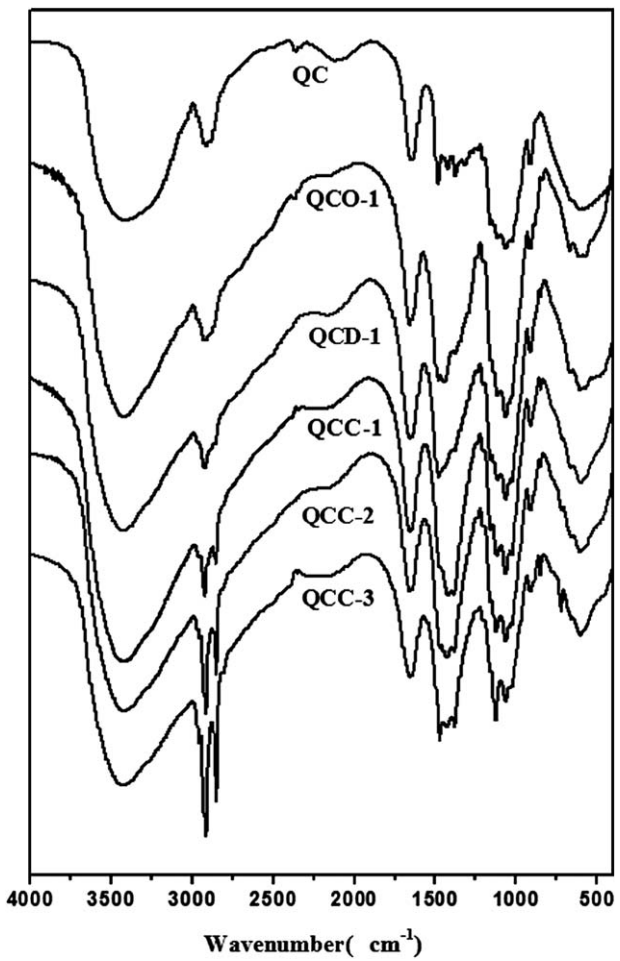

Fig. 1 FT-IR spectra of the QC and HMQC derivatives.

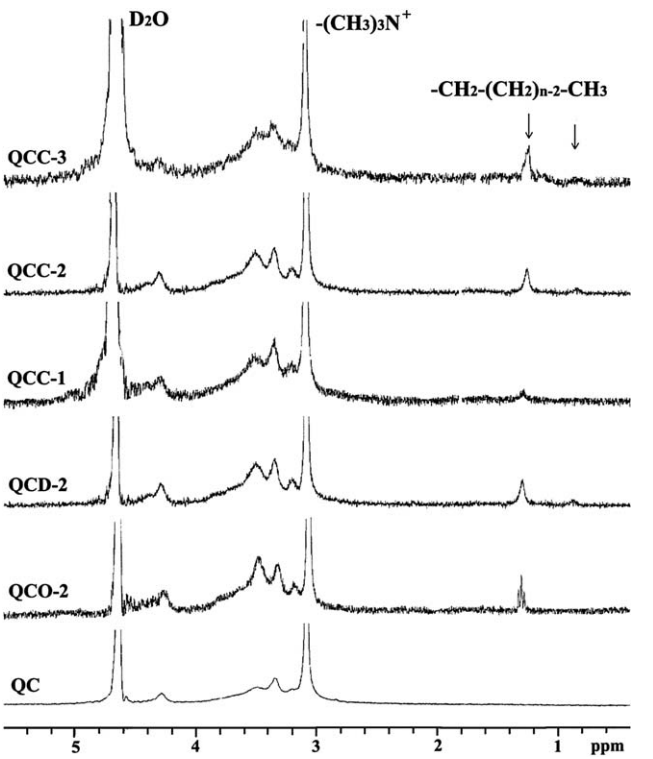

Fig. 2 ^1H NMR spectra of the QC and HMQC derivatives.

DS_H value. Therefore, from the results of the FT-IR and ^1H NMR, the long alkyl chain was successfully conjugated to the backbone of the quaternized cellulose.

3.2 Formation and physicochemical properties of micelles

The introduction of the quaternary ammonium as hydrophilic segments and long alkyl groups as hydrophobic segments to the backbone of the cellulose provided the opportunity to form micelles in distilled water. Our previous work had proved the formation of these micelles by a fluorescence technique, using pyrene as a probe.[26] The CMC is a very important parameter for polymeric micelles and defines the thermodynamic stability of the micelles.[30] The amphiphilic polymers could only self-assemble into micelles above the CMC, in aqueous solution.[34–36] As shown in Table 1, the CMC values of QCO-1, QCO-2, and QCO-3 were 648.9, 301.1 and 207.0 mg L^{-1}, respectively, which decreased as the DS_H increased. The CMC value was decreased as the length of the alkyl groups increased for the same DS_H value of the HMQC (QCO-2, QCD-2 and QCC-3). The higher degree of hydrophobic substitution and lengthening of the long alkyl chain of the polymeric micelles can lead to a lower CMC value. The ζ-potential values of the HMQC micelles in water are also listed in Table 1. The ζ-potential of micelles was about 50 mV, which was slightly higher than that of the QC in water (48.4 mV). The cationic surface charge of the micelles could promote an interaction of the micelles with the cells and hence increase the rate and extent of internalization.[37]

Fig. 3 shows the hydrodynamic radius (R_h) distribution of the QCC micelles and BTPETD-loaded QCC-3 micelles in distilled water. The R_h values for QCC-1, QCC-2, and QCC-3 were 322.6, 246.8 and 229.2 nm, respectively, which decreased as the DS_H value increased. It suggested that the more hydrophobic long alkyl chains had strengthened the hydrophobic interaction of the micelle core. The R_h values for all the HMQC micelles are listed in Table 1. The R_h values decreased as the length of the alkyl chain decreased. The hydrophobic interaction was strengthened to obtain a lower R_h value by shortening the hydrophobic chain and increasing the DS_H, leading to a tighter core for the micelles. Moreover, the R_h of the micelles decreased with an increase in the NaCl concentration from 0 to 0.5 mol L^{-1}, and then hardly changed with a further increase in the ionic strength of the solution. When the BTPETD was encapsulated into the QCC-3 micelles, the R_h value was slightly decreased compared with those of the dye-free micelles, due to the enhanced hydrophobic interaction between the hydrophobic dyes and the micelle cores.

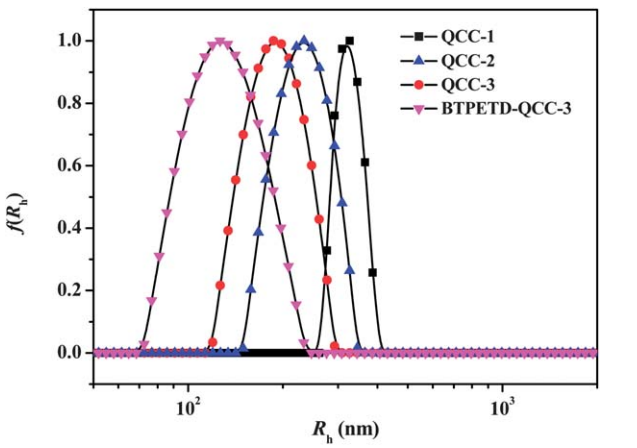

Fig. 3 Hydrodynamic radius (R_h) distribution of the QCC micelles and the BTPETD-loaded QCC-3 micelles in aqueous solution.

To better understand the formation of the self-assembled micelles, their morphologies were observed by TEM (Fig. 4). As illustrated, the self-assembled micelles were individual nanoparticles with a regular spherical shape, and dispersed homogeneously, attributed to the cationic outer shells. From the TEM images (Fig. 4a–c), the average sizes of the QCC micelles were 42.5, 40.7 and 37.6 nm, which decreased as the DS_H increased. The average sizes of QCD-2 (Fig. 4d) and QCO-2 (Fig. 4e) were 30.4 and 27.2 nm, respectively, decreasing as the length of the hydrophobic chains decreased. Besides, these were much smaller than those observed by DLS, mainly attributed to the fact that the hydrophilic backbone of the micelles tends to shrink during the drying process of TEM sample preparation. Similar to the observations from DLS, the size of the BTPETD-loaded QCC-3 micelles (36.3 nm, Fig. 4f) were slightly smaller than those of the dye-free micelles.

3.3 Fluorescent properties of BTPETD-loaded micelles

The fluorescent micelles were prepared by assembling the BTPETD molecules into the core of the HMQC micelles. A schematic representation of HMQC micelles and the BTPETD-loaded micelles is depicted in Scheme 2. Driven by hydrophobic interactions, the amphiphilic HMQC tends to self-assemble into micelles with hydrophobic cores and hydrophilic shells. The core is formed by alkyl segments, which can act as a reservoir for accommodating the hydrophobic fluorescent BTPETD. The BTPETD-loaded micelles in aqueous solution turned yellow upon UV irradiation, while BTPETD dissolved in DMSO turned orange. Fig. 5 compares the UV-vis and fluorescent spectra of the BTPETD in DMSO and the BTPETD-loaded QCC-1 micelles in water. The BTPETD exhibits an absorbance peak at 415 nm with the corresponding fluorescent emission peak at 563 nm in DMSO. In an aqueous solution of QCC-1 micelles, the BTPETD shows a similar absorbance main peak at around 426 nm. Consequently, the fluorescent spectra of BTPETD-loaded micelles in water exhibits a large blue-shift from the spectrum at 533 nm, which can be attributed to the change in the chain conformation or increased inter and intra-chain interactions of BTPETD in the hydrophobic micelle core. Meanwhile, a better photoluminescent property was observed after the BTPETD was assembled into the core of the micelles.

The loading capacity (LC) and loading efficiency (LE) of the BTPETD in HMQC micelles are listed in Table 2. The LE and LC values of the QCC micelles increased as the DS_H increased, and with increased length of alkyl chain at the same DS_H. This was ascribed to the more hydrophobic moiety and the stronger interaction between the HMQC micelle core and the hydrophobic BTPETD dye. The fluorescence quantum yield (Φ_F) of the

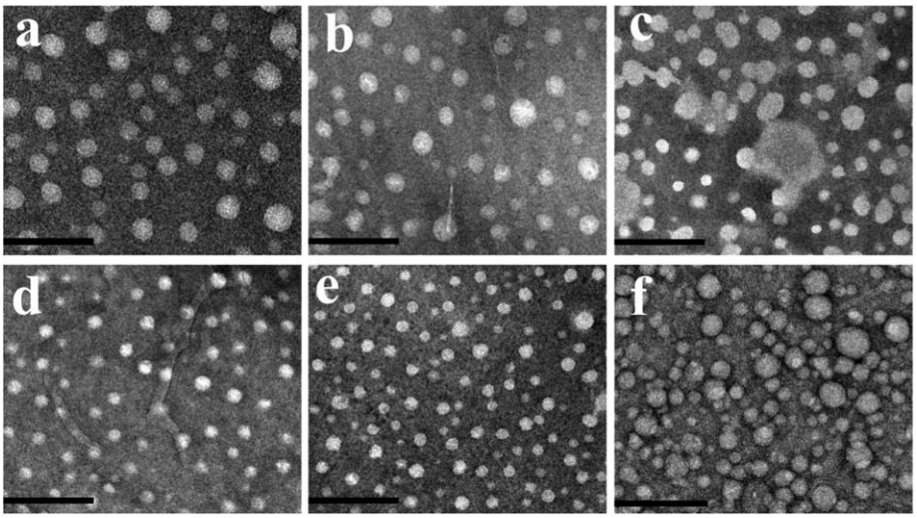

Fig. 4 TEM images of the self-assembled HMQC micelles: (a) QCC-1, (b) QCC-2, (c) QCC-3, (d) QCD-2, (e) QCO-2 and (f) BTPETD-loaded QCC-3 micelles. The scale bar is 200 nm.

BTPETD was 0.256. When loaded into the HMQC micelles, the values of Φ_F were larger than that of the BTPETD in DMSO. As shown in Table 2, the quantum yield increased with increasing length of the alkyl chain, but decreased with increasing DS_H value.

3.4 Sensing properties for explosives

The tetraphenylethene derivative (d-TPE) presents a good electron donor ability. Due to this intrinsic electron donating capability, d-TPE could be a promising sensor material to detect nitroaromatic explosives.[2,12,15] Herein, the selectivity of this fluorescent BTPETD-loaded HMQC micelles detection system for TNT, PA and other nitro compounds, such as NP, NT, DNP and DNT was investigated. Fig. 6 presents the relative fluorescence quenching efficiencies of the fluorescent BTPETD-loaded QCD-2 micelles in the presence of 25 μM of the nitro compounds. We found the fluorescence quenched by DNP and PA was higher than that by the other nitro compounds. The fluorescence quenching efficiencies caused by NP, NT, DNP, DNT, PA and TNT were about 4.20, 13.98, 80.12, 32.90, 95.95 and 42.51%, respectively. The BTPETD-loaded micelle has excellent selectivity toward PA over the other tested nitroaromatic compounds.

Fig. 7a and c show the fluorescence spectra of the BTPETD-loaded QCD-2 micelles upon exposure to DNP and PA in aqueous solution, respectively. The fluorescence intensity was significantly quenched when 25 μM of DNP was added. However, a similar but much more profound quenching effect was observed in the fluorescent properties of the BTPETD-loaded QCD-2 micelles in response to PA. When 25 μM of PA was added to the BTPETD-loaded micelles solution, the fluorescence intensity was almost completely quenched. This phenomenon was ascribed to the lower LUMO energy level of PA.[17,38] When an electron deficient molecule, such as PA is present, an electron-transfer quenching could occur from the excited BTPETD to the LUMO of the analyte. Moreover, the quenching process was very fast, and the quenching equilibrium could be reached in 10 s.

The Stern–Volmer equation was used to quantify the quenching efficiency:[7,39,40]

$$I_0/I = 1 + K_{SV} \times c \quad (5)$$

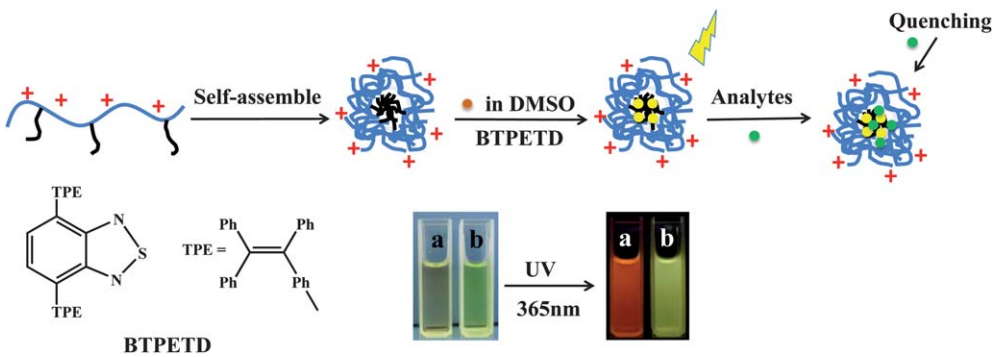

Scheme 2 Schematic representation and photographs of the HMQC micelles and BTPETD-loaded HMQC micelles: (a) the BTPETD solution in DMSO, and (b) the BTPETD-loaded micelles in aqueous solution; both the solutions are with a BTPETD concentration of 0.01 mg mL^{-1}.

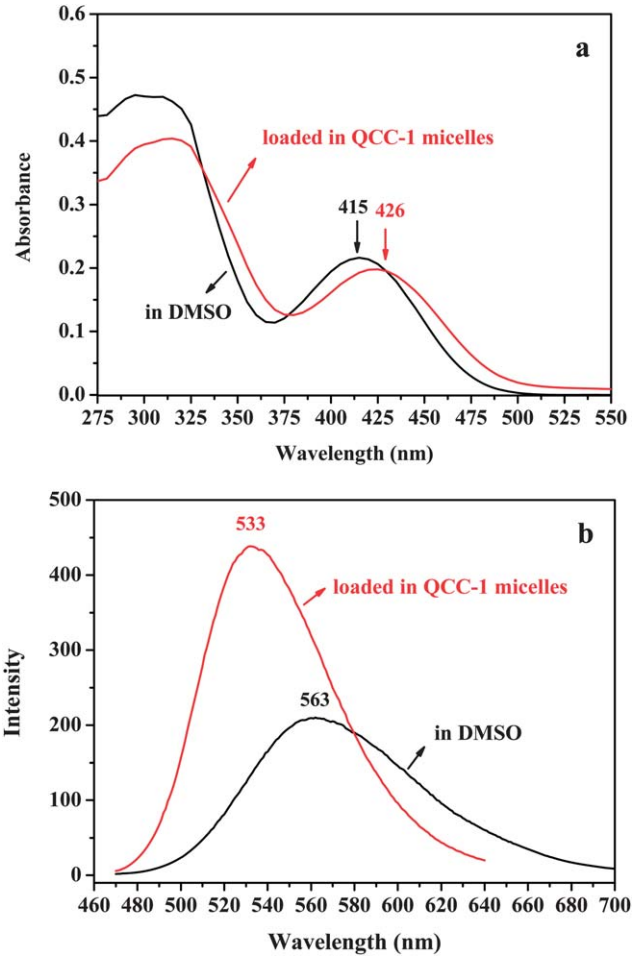

Fig. 5 (a) UV-vis and (b) fluorescent spectra of the BTPETD in DMSO and the BTPETD-loaded QCC-1 micelles in an aqueous solution. The concentration of BTPETD is 0.01 mg mL^{-1}.

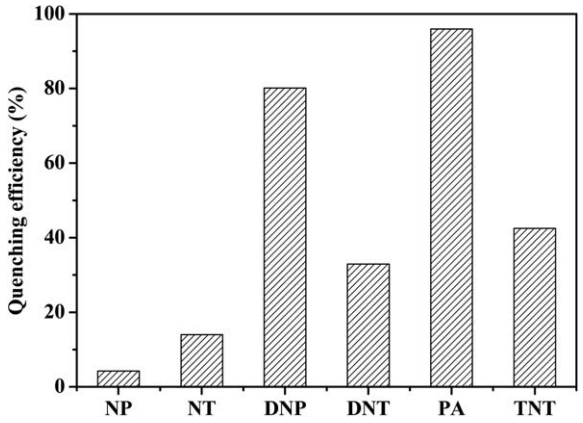

Fig. 6 The relative fluorescence quenching efficiencies of the BTPETD-loaded QCD-2 micelles in the presence of 25 μM of the nitrocompounds.

where I_0 is the initial fluorescence intensity without the analyte, I is the fluorescence intensity with the added analyte of concentration (c), and K_{SV} is the Stern–Volmer constant. Fig. 7b and d display the Stern–Volmer plots of the BTPETD in DMSO and the BTPETD-loaded QCD-2 micelles for DNP and PA. A linear relationship is observed in all cases for the fluorescence quenching by DNP. Compared to the BTPETD in DMSO, a more upward plot was obtained on the BTPETD-loaded QCD-2 micelles, which means a better effective quenching. The K_{SV} values for the BTPETD in DMSO and the BTPETD-loaded QCD-2 by DNP were 0.289×10^5 and 1.577×10^5 M^{-1} (Table 2), respectively. The value of K_{SV} could also be used to represent the quenching efficiency; for higher values of K_{SV}, a better quenching is obtained. For quenching by PA, the Stern–Volmer plot is more superlinear for $c \geq 6$ μM, because one of the BTPETD molecules may simultaneously combine with more PA, which causes a rapid and great reduction of the fluorescence intensity. A linear relationship from $(I_0' - I')/I' \sim \log c$ was obtained and the equation is shown as follows:

$$I_0'/I' = 1 + K_{SV}' \times c \text{ for } c < 6\ \mu M \quad (6)$$

$$(I_0' - I')/I' = a + K_{PA} \times \log c \text{ for } c \geq 6\ \mu M \quad (7)$$

where I_0' is the initial fluorescence intensity without the analyte, I' is the fluorescence intensity with the added analyte of concentration (c), K_{SV}' is the Stern–Volmer quenching constant when $c < 6$ μM, K_{PA} is the constant for eqn (7), and a is the intercept. The values of K_{SV}' and K_{PA} are shown in Table 2. The quenching constant for the BTPETD-loaded QCD-2 by PA was higher than that in DMSO, which means a profound quenching effect was obtained. The K_{SV} and K_{SV}' values increased as the DS_H increased, and also increased upon lengthening the hydrophobic alkyl chain with the same DS_H, because of the higher LC values of the QCC micelles. However, for K_{PA}, it is just the opposite compared to K_{SV} and K_{SV}'. Therefore, the explosives

Table 2 Loading capacity (LC), loading efficiency (LE), fluorescence quantum yield (Φ_F) and quenching constants of the BTPETD in DMSO and BTPETD-loaded HMQC micelles

Sample	LC (%)	LE (%)	Φ_F	K_{SV} for DNP ($\times 10^5$ M^{-1})	K_{SV}' for PA ($\times 10^5$ M^{-1})	K_{PA}
BTPETD	—	—	0.256	0.289	2.271	0.551
QCO-2	8.36	62.71	0.357	0.198	2.046	0.661
QCD-2	10.57	79.25	0.424	1.577	2.435	0.566
QCC-1	11.25	84.41	0.554	0.665	2.616	0.544
QCC-2	11.34	85.06	0.536	2.143	3.076	0.460
QCC-3	11.57	86.80	0.435	2.631	3.634	0.430

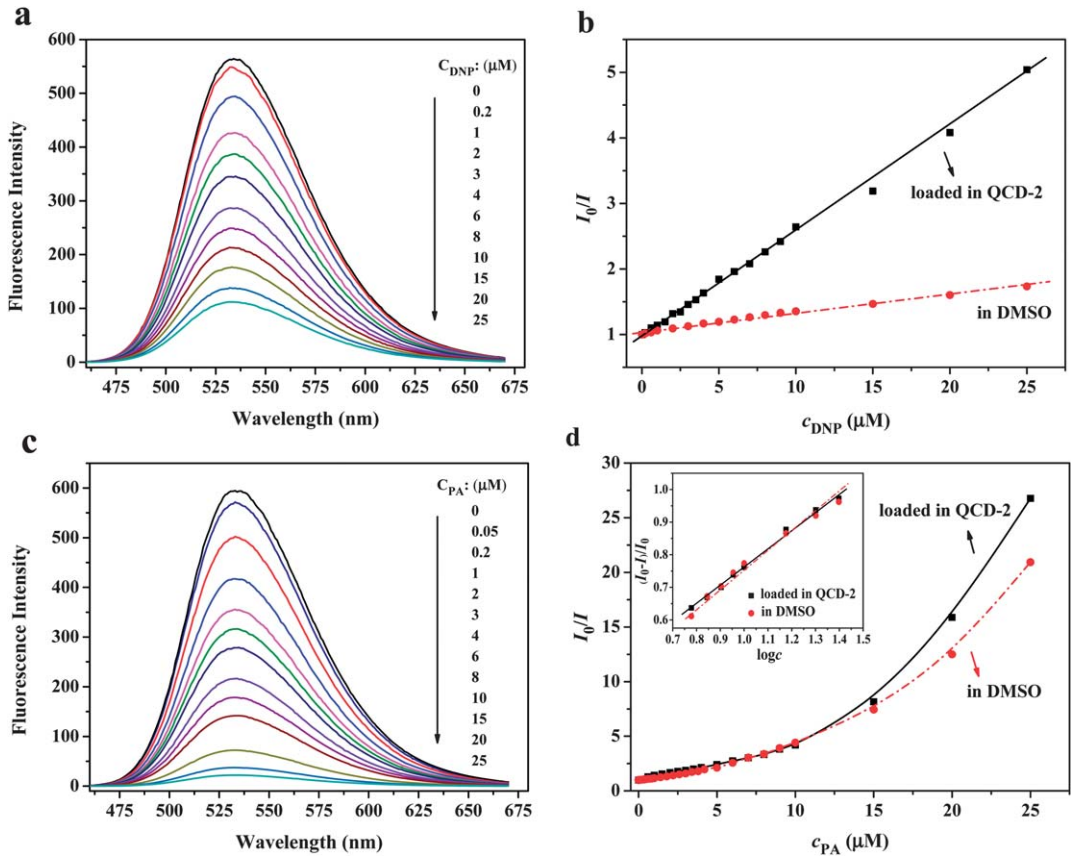

Fig. 7 Fluorescence emission spectra of the BTPETD-loaded QCD-2 in water in the presence of (a) DNP and (c) PA. Stern–Volmer plots for the BTPETD in DMSO and the BTPETD-loaded QCD-2 micelles in water with the analytes of (b) DNP and (d) PA.

could be quantitatively detected by fluorescence quenching, and the limit of detection could reach 200 and 50 nM for DNP and PA, respectively. Moreover, the sensing results were barely influenced by the ionic strength of the solution. With its high stability and sensitivity to DNP and PA, the fluorescent cellulose micelle is a good chemosensing system in aqueous solution, and has potential applications.

4 Conclusions

In summary, a series of quaternized cellulose derivatives with different hydrophobic long alkyl chains were successfully prepared. They could be self-assembled into micelles to load hydrophobic dyes into the hydrophobic cores. Therefore, a novel chemosensing system based on fluorescent cellulose micelles was obtained, and displayed excellent photoluminescent properties and a highly fluorescence quenching sensitivity in the presence of DNP and PA. The excited state electron transfer from the electron rich fluorescent molecules to the electron deficient nitroaromatics was probably the mechanism to cause the quenching. The fluorescence intensity has a good linear relationship to DNP detection, while being superlinear for $c \geq 6$ μM to PA detection, and both of them can be quantitatively detected. Therefore, the BTPETD-loaded cellulose micelles exhibited potential for the preparation of feasible, sensitive and stable sensor materials for detecting explosives in aqueous solution. Moreover, the amphiphilic cellulose micelles as renewable, abundant and biocompatible media have promise for extending their applications, such as in detecting or biological imaging.

Acknowledgements

This work was financially supported by the National Natural Science Foundation of China (50973085 and 51273151), the Program for New Century Excellent Talents in University (NCET-11-0415) and the National Basic Research Program of China (973 Program, 2010CB732203). J. Z. thanks the Japan Society for the Promotion of Science (JSPS) Invitation Fellowship for Research in Japan for the financial support.

Notes and references

1 H. Li, J. X. Wang, Z. L. Pan, L. Y. Cui, L. Xu, R. M. Wang, Y. L. Song and L. Jiang, *J. Mater. Chem.*, 2011, **21**, 1730–1735.
2 X. D. Yang, B. W. Shen, Y. N. Jiang, Z. X. Zhao, C. X. Wang, C. Ma, B. Yang and Q. Lin, *J. Mater. Chem. A*, 2013, **1**, 1201–1206.
3 Y. Engel, R. Elnathan, A. Pevzner, G. Davidi, E. Flaxer and F. Patolsky, *Angew. Chem., Int. Ed.*, 2010, **49**, 6830–6835.

4 S. S. R. Dasary, D. Senapati, A. K. Singh, Y. Anjaneyulu, H. T. Yu and P. C. Ray, *ACS Appl. Mater. Interfaces*, 2010, **2**, 3455–3460.
5 M. Riskin, R. Tel-Vered, O. Lioubashevski and I. Willner, *J. Am. Chem. Soc.*, 2009, **131**, 7368–7378.
6 A. Rose, Z. G. Zhu, C. F. Madigan, T. M. Swager and V. Bulovic, *Nature*, 2005, **434**, 876–879.
7 S. W. Thomas, G. D. Joly and T. M. Swager, *Chem. Rev.*, 2007, **107**, 1339–1386.
8 L. H. Tang, H. B. Feng, J. S. Cheng and J. H. Li, *Chem. Commun.*, 2010, **46**, 5882–5884.
9 A. D. Aguilar, E. S. Forzani, M. Leright, F. Tsow, A. Cagan, R. A. Iglesias, L. A. Nagahara, I. Amlani, R. Tsui and N. J. Tao, *Nano Lett.*, 2010, **10**, 380–384.
10 K. Zhang, H. B. Zhou, Q. S. Mei, S. H. Wang, G. J. Guan, R. Y. Liu, J. Zhang and Z. P. Zhang, *J. Am. Chem. Soc.*, 2011, **133**, 8424–8427.
11 T. L. Andrew and T. M. Swager, *J. Am. Chem. Soc.*, 2007, **129**, 7254–7255.
12 D. T. McQuade, A. E. Pullen and T. M. Swager, *Chem. Rev.*, 2000, **100**, 2537–2574.
13 M. S. Meaney and V. L. McGuffin, *Anal. Chim. Acta*, 2008, **610**, 57–67.
14 H. Nie, Y. Zhao, M. Zhang, Y. G. Ma, M. Baumgartenb and K. Müllen, *Chem. Commun.*, 2011, **47**, 1234–1236.
15 J. S. Yang and T. M. Swager, *J. Am. Chem. Soc.*, 1998, **120**, 5321–5322.
16 D. H. Zhao and T. M. Swager, *Macromolecules*, 2005, **38**, 9377–9384.
17 B. W. Xu, X. F. Wu, H. B. Li, H. Tong and L. X. Wang, *Macromolecules*, 2011, **44**, 5089–5092.
18 X. H. Wang, Y. Z. Guo, D. Li, H. Chen and R. C. Sun, *Chem. Commun.*, 2012, **48**, 5569–5591.
19 D. Klemm, B. Heubletin, H.-P. Fink and A. Bohn, *Angew. Chem., Int. Ed.*, 2005, **44**, 3358–3393.
20 A. G. Cunha and A. Gandini, *Cellulose*, 2010, **17**, 875–889.
21 L. J. Nielsen, S. Eyley, W. Thielemans and J. W. Aylott, *Chem. Commun.*, 2010, **46**, 8929–8931.
22 H. J. Dou, M. Jiang, H. S. Peng, D. Y. Chen and Y. Hong, *Angew. Chem., Int. Ed.*, 2003, **42**, 1516–1519.
23 H. L. Kang, W. Y. Liu, B. Q. He, D. W. Shen, L. Ma and Y. Huang, *Polymer*, 2006, **47**, 7927–7934.
24 S. Wan, M. Jiang and G. Z. Zhang, *Macromolecules*, 2007, **40**, 5552–5558.
25 T. Akagi, M. Baba and M. Akashi, *Polymer*, 2007, **48**, 6729–6747.
26 Y. Song, L. Zhang, W. Gan, J. Zhou and L. Zhang, *Colloids Surf., B*, 2011, **83**, 313–320.
27 S. J. Toal and W. C. Trogler, *J. Mater. Chem.*, 2006, **16**, 2871–2883.
28 Z. Zhao, C. Deng, S. Chen, J. W. Y. Lam, W. Qin, P. Lu, Z. Wang, H. S. Kwok, Y. Ma, H. Qin and B. Z. Tang, *Chem. Commun.*, 2011, **47**, 8847–8849.
29 Y. Song, Y. Sun, X. Zhang, J. Zhou and L. Zhang, *Biomacromolecules*, 2008, **9**, 2259–2264.
30 N. Rapoport, *Prog. Polym. Sci.*, 2007, **32**, 962–990.
31 P. Meallier, S. Guittonneau, C. Emmelin and T. Konstantinova, *Dyes Pigm.*, 1999, **40**, 95–98.
32 C. Zhang, Q. Ping, H. Zhang and J. Shen, *Carbohydr. Polym.*, 2003, **54**, 137–141.
33 T. Heinze, S. Rensinga and A. Koschella, *Starch/Staerke*, 2007, **59**, 199–207.
34 A. N. Lukyanov and V. P. Torchilin, *Adv. Drug Delivery Rev.*, 2004, **56**, 1273–1289.
35 D. E. Discher and A. Eisenberg, *Science*, 2002, **297**, 967–973.
36 M. Antonietti and S. Förster, *Adv. Mater.*, 2003, **15**, 1323–1333.
37 A. Kumari, S. K. Yadav and S. C. Yadav, *Colloids Surf., B*, 2010, **75**, 1–18.
38 H. Sohn, M. J. Sailor, D. Magde and W. C. Trogler, *J. Am. Chem. Soc.*, 2003, **125**, 3821–3830.
39 C. B. Murphy, Y. Zhang, T. Troxler, V. Ferry, J. J. Martin and W. E. Jones Jr, *J. Phys. Chem. B*, 2004, **108**, 1537–1543.
40 J. R. Lakowicz, *Principles of Fluorescence Spectroscopy*, Plenum Press, New York, 2nd edn, 1999.

